SUPPLEMENTARY INFORMATION

TRPC channel activation by extracellular thioredoxin

Shang-Zhong Xu[1*], Piruthivi Sukumar[1*], Fanning Zeng[1], Jing Li[1], Amit Jairaman[1], Anne English[3], Jacqueline Naylor[1], Coziana Ciurtin[1], Yasser Majeed[1], Carol J Milligan[1], Yahya M Bahnasi[1], Eman AL-Shawaf[1], Karen E Porter[2], Lin-Hua Jiang[1], Paul Emery[3], Asipu Sivaprasadarao[1], David J Beech[1]

[1]Institute of Membrane & Systems Biology, Garstang Building, Faculty of Biological Sciences and [2]School of Medicine, University of Leeds, Leeds, LS2 9JT, UK. [3]Academic Unit of Musculoskeletal Disease, Chapel Allerton Hospital, Leeds LS7 4SA. *These authors contributed equally to this work.

SUPPLEMENTARY METHODS

Ca^{2+} imaging. Cells were preincubated with 1 μM fura PE3-AM at 37 °C for 1 hr in standard bath solution, followed by 15-30 min in standard bath solution at room temperature. Fura-PE3 was excited alternately by 340 and 380 nm light and emission was collected via a 510-nm filter and sampled by a CCD camera (Orca ER). Images were sampled every 10 s in pairs for the two excitation wavelengths and ratios produced using regions of interest to select individual cells. Imaging was controlled by Openlab 2.0 software. Experiments were at room temperature. The *n* values given are the number cells from at least three independent experiments.

TRPC6 and TRPM2 expression and recording. HEK-293 cells stably expressing TRPC6 (from G Boulay) have been described[1]. Recording conditions were the same as described for

TRPC5 recording in the absence of Gd^{3+}. TRPM2 expression and recording has been described.[2] Briefly: Recordings were made using bath solution containing (mM) 145 NaCl, 2 KCl, 13 D-glucose, 10 HEPES, 1 $MgCl_2$, 2 $CaCl_2$, pH adjusted to 7.3 with NaOH. The patch pipette solution contained (mM) 145 NaCl, 0.05 EGTA, 1 Na_2ATP, 1 ADP-ribose, pH adjusted to 7.3 with NaOH.

Western blotting. The protocol was similar to that described previously[3]. Cells were placed in PBS containing protease inhibitor cocktail (Sigma) and lysed in Laemmli buffer with or without 1 mM dithiothreitol at 80 °C to 100 °C (15 min). Proteins were separated on 8 % SDS-PAGE gels and transferred to nitrocellulose membrane (Millipore) and probed with custom-made rabbit anti-TRPC5 (T5C3, 1:100 dilution) antibody[4] or anti-TRPC1 (T1E3, 1:500 dilution) antibody[3]. Secondary antibody was conjugated with horseradish peroxidase. Membranes were washed with PBS and labelling detected by ECLplus (Amersham).

RNA isolation and RT-PCR. Total RNA was isolated from FLS cells using a standard TriReagent protocol and treated with DNAse I (Ambion). An aliquot of this RNA was used for cDNA synthesis with oligo-dT primed AMV reverse transcriptase ("+RT") and another was processed in parallel except for the omission of reverse transcriptase ("-RT"). PCR primer sequences were (forward and reverse, 5'-3'): TRPC1 (TGGTATGAAGGGTTGGAAGAC and GGTATCATTGCTTTGCTGTTC); TRPC5 (CATGACTGGTGGAACC and ATGAGAGTTGGCTGTGAA); Primers were used at 0.5 μM and with 3 mM Mg^{2+}. Thermal cycling was 40 cycles of: 94 °C (30 s); 56.6 °C (1 min); 72 °C (1 min). TRPC5 mRNA was detected after the first 40 cycles but a second round of PCR was used to increase the quantity of product for presentation purposes. Parallel control reactions were always performed in the absence of reverse transcriptase and no products were detected in these controls. PCR products were electrophoresed on 1.5 % agarose gels containing ethidium bromide. Direct sequencing confirmed the identity of products.

Short interfering (si) RNA. 0.5-2 x10^6 human FLS cells were centrifuged (100 g) for 10 min, resuspended in Basic Nucleofector solution (Amaxa), mixed with 1 μM siRNA (Ambion) and transferred into a cuvette for electroporation (Amaxa). Cells were transferred from cuvettes to pre-warmed culture medium and incubated in a 5 % CO_2 incubator at 37 ^oC. Culture medium was changed after 24 hr and measurements were made after a further 24 hr. Highly efficient transfection could not be achieved (experiments with a Cy3-labelled siRNA indicated 30-40 % of cells were transfected). TRPC siRNA probes were (5'-3': only single strands are shown): GCCCGGAAUUCUCGUGAAUtt for TRPC1; and GCAACCUUGGGCUGUUCAUtt for TRPC5. Cells were simultaneously transfected with both probes (0.5 μM each). The siRNA control was Silencer Negative Control #1 siRNA (Ambion catalogue number 4611), which is a 19 bp scrambled sequence with 3' dT overhangs and having no significant homology to any known human gene sequences (Ambion). Effectiveness of TRPC1/5 siRNA probes was validated using quantitative real-time RT-PCR. PCR primers for measuring mRNA abundances were (forward and reverse, 5'-3'): TRPC1 (TTAGCGCATGTGGCAA and CCACTTACTGAGGCTACTAAT); TRPC5 (ACATTTTAAGTTCGTTGCG and ACATCGGATCCCCTTG); STIM1 (CTCTCTTGACTCGCCA and GCTTAGCAAGGTTGATCT); β-actin (TCGAGCAAGAGATGGC and TGAAGGTAGTTTCGTGGATG).

Isometric tension recordings. Eight week old male C57/BL6 mice were killed by CO_2 asphyxiation and cervical dissociation in accordance with the Code of Practice, UK Animals Scientific Procedures Act 1986. Recordings were made from rings of mouse aorta as previously described[5].

Chemicals. Carbachol and S-nitroso-N-acetylpenicillamine (SNAP) were from Sigma. Fura-PE3 AM was from Invitrogen.

SUPPLEMENTARY FIGURES

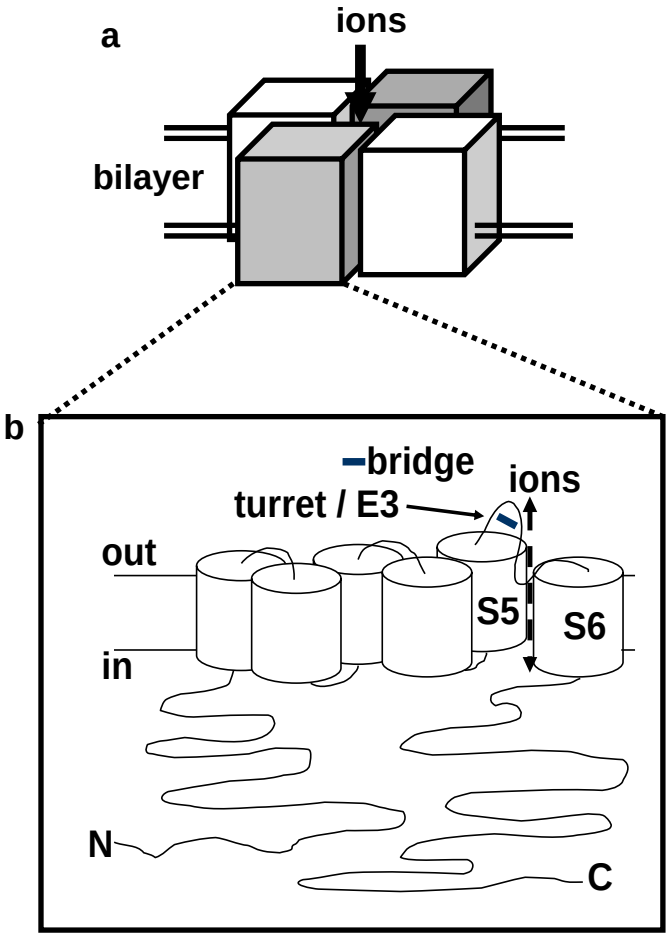

Supplementary Fig. 1| Schematic showing the presumed elementary structure of a TRP channel. a, Tetrameric arrangement in the plasma membrane. Each block represents one TRP protein. Heteromultimers may occur, for example between TRPC1 and TRPC5[4,6]. Ion conduction is gated by structural elements in the TRPC proteins and occurs through a central pore. **b,** Proposed membrane topology of one TRP protein. Amino (N) and carboxy (C) termini are intracellular and there are six membrane-spanning segments (the 5th and 6th are marked S5 and S6). The predicted extracellular loop at the top of S5, near the ion pore, has been referred to as the turret in other related ion channels[7]. In our predictions for generation of blocking antibodies the region is referred to as E3, the third extracellular loop[8]. We hypothesise that breaking of a disulphide bridge (**-**) in the loop leads to increased current in channels containing TRPC5 or an equivalent subunit.

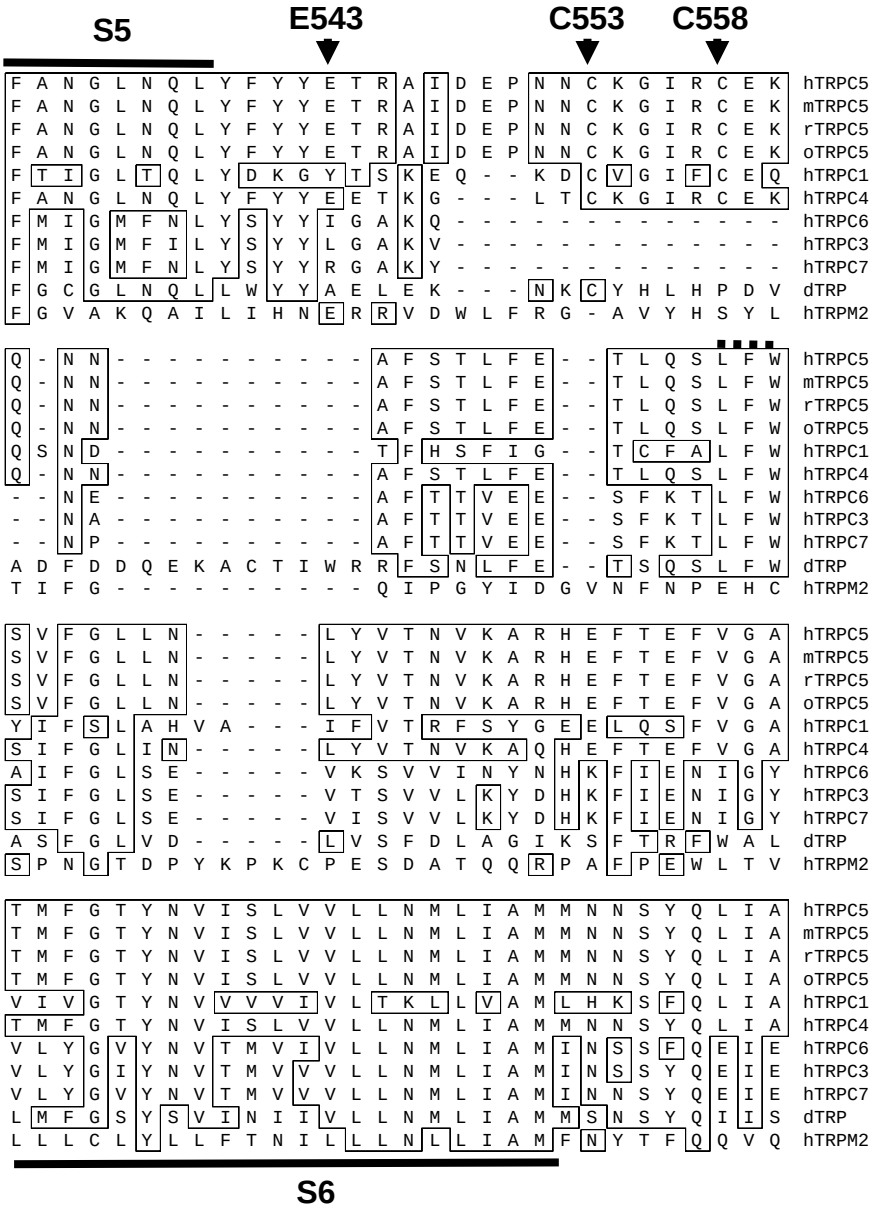

Supplementary Fig. 2| Sequence alignment in the S5-S6 loop region. Entire amino acid sequences of eleven TRP channels were aligned (Clustal W software) but only predicted S5-to-S6 regions are shown. The conserved LFW sequence (marked with a broken line) is thought to reside in the ion-pore and is used as validation for the alignment, along with the LIAM sequence at the end of S6. Cysteines 553 and 558 of TRPC5 are indicated. E543 is involved in the agonist action of lanthanides[9]. We consider the predicted extracellular loop in question (the "turret") as amino acids between S5 and LFW. Abbreviations: h, human; m, mouse; r, rat; o, *oryctolagus cuniculus* (rabbit); d, *drosophila melanogaster* (fruit fly).

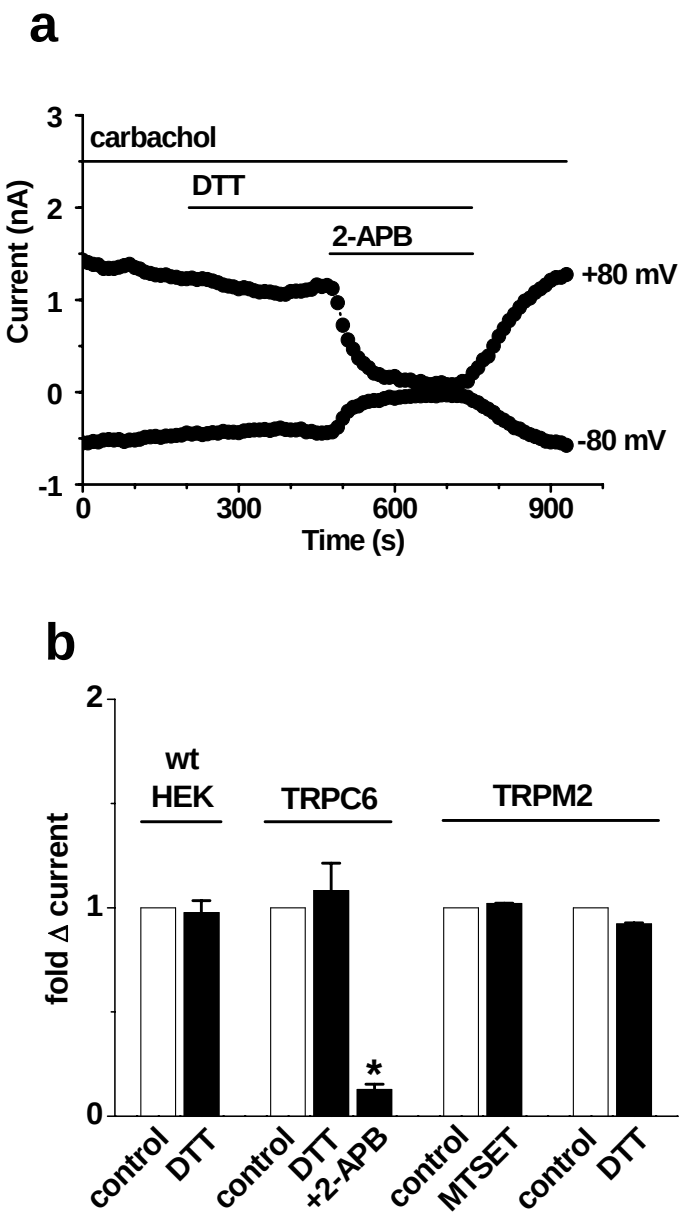

Supplementary Fig. 3| Lack of effect of dithiothreitol (DTT) on TRPC6 or TRPM2. Whole-cell voltage-clamp recordings were made from HEK 293 cells over-expressing TRPC6, TRPM2 or neither. **a**, Example recording from a TRPC6-expressing cell. Carbachol (0.1 mM), dithiothreitol (DTT, 10 mM) and 2-APB (75 μM) were bath-applied. Current was sampled every 10 s at +80 mV and -80 mV from the ramp protocol. **b**, Mean fold change (Δ) in current at –80 mV in wild-type (wt) HEK cells (*n*=5) or HEK cells expressing TRPC6 (*n*=7) or TRPM2 (MTSET, *n*=4; DTT, *n*=3). A fold change of 1.0 indicates no change.

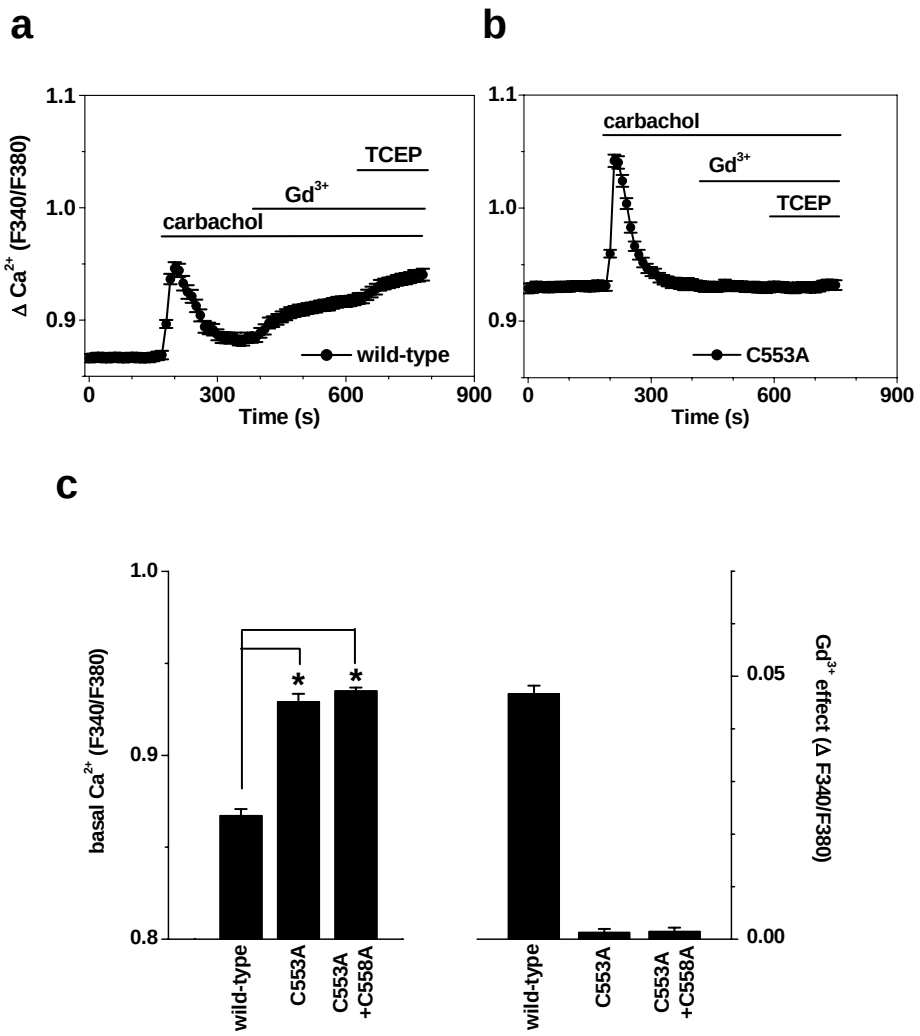

Supplementary Fig. 4| Intracellular calcium measurements from cells expressing cysteine mutants. HEK 293 cells were transiently transfected with wild-type TRPC5, the C553A single mutant of TRPC5, or the C553A+C558A double mutant. All recordings were in standard bath solution and intracellular Ca^{2+} was indicated by the fura-PE3 fluorescence ratio. **a, b,** Examples showing effects of serial additions of extracellular 0.1 mM carbachol, 0.1 mM gadolinium ions (Gd^{3+}) and 1 mM TCEP. Basal Ca^{2+} is higher for the mutant and responses to Gd^{3+} and TCEP are lacking. The transient response to carbachol is Ca^{2+}-release from intracellular stores and not an indicator of TRPC5 activity. (**c**) Mean data (cell number, 60-111) showing basal Ca^{2+} (on the left) and the change in Ca^{2+} evoked by Gd^{3+} (on the right), as illustrated in (**a-b**).

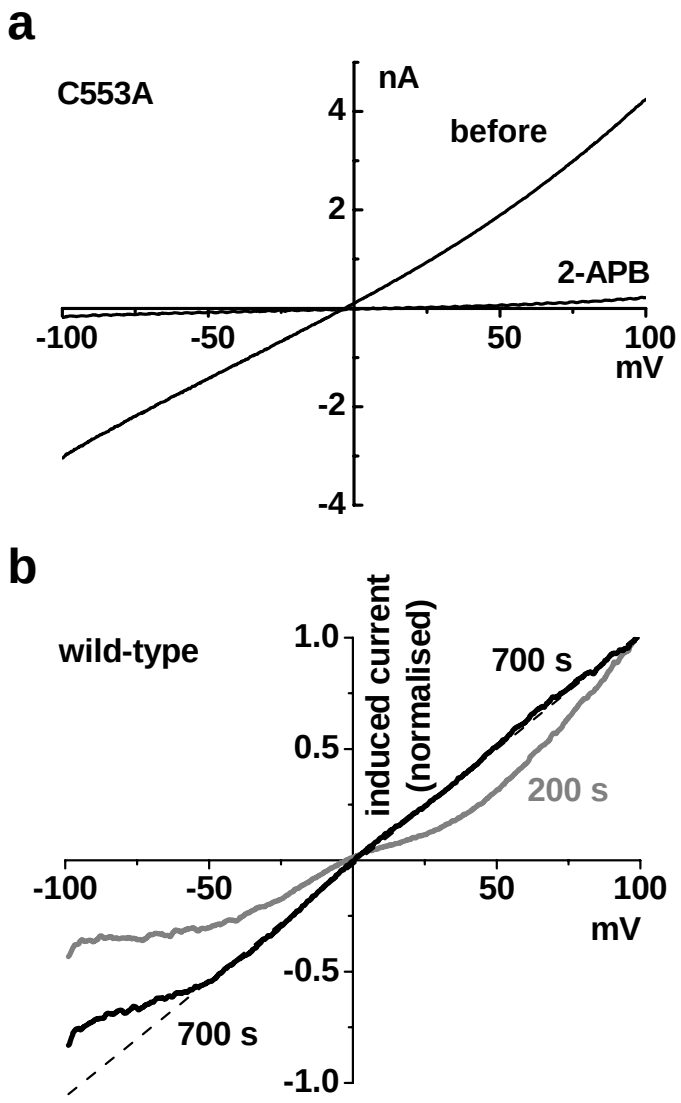

Supplementary Fig. 5| Current-voltage relationships (I-Vs) of cysteine mutants. Whole-cell voltage-clamp recordings from HEK 293 cells over-expressing C553A (**a**) or wild-type (**b**) TRPC5. I-Vs were produced using the -100 to +100 mV ramp protocol. **a**, The I-V is shown before and after bath-application of 75 μM 2-APB. The I-Vs for the C553A, C553S, C558A and C553A+C558A mutants were similar and all were blocked by 2-APB (data not shown). **b**, The DTT-evoked I-V is shown 200 s (grey) and 700 s (black) after bath-application of 1 mM DTT. The dashed line is a straight line fitted to the current at 700 s, showing the I-V is linear apart from residual rectification negative of -50 mV. **a, b**, The data show the I-Vs of the tonically active cysteine mutants are linear, lacking the characteristic

double-rectifying shape of the wild-type TRPC5 (eg *cf* Fig 1b). The data also show that this effect can be reasonably well reproduced by prolonged exposure of the wild-type TRPC5 to DTT. The latter experiment was difficult to perform because of the deleterious effect of prolonged exposure of the entire cell to high concentrations of DTT. We hypothesise that the linear I-V is characteristic of TRPC5 when there is complete absence of disulphide bridges in the extracellular loop, as there is for the cysteine mutants. The data suggest that complete disruption of the bridge in the turret reduces voltage-dependence of the channel. The reason for this effect is unknown but one possibility is allosteric interaction between the extracellular cysteine residues and the aspartic acid residue involved in magnesium-dependent rectification[10].

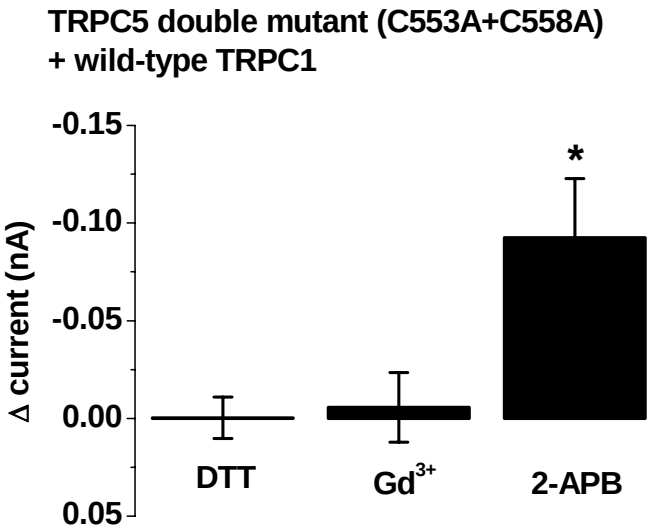

Supplementary Fig. 6| Inability of cysteine residues in TRPC1 to compensate for lack of cysteine residues in TRPC5. Mean change in current at -80 mV in whole-cell recordings from HEK 293 cells co-expressing wild-type TRPC1 with the double mutant TRPC5 C553A+C558A (*n*=5 for each). There was no response to 10 mM DTT or 100 μM Gd^{3+}, but current was inhibited by 75 μM 2-APB.

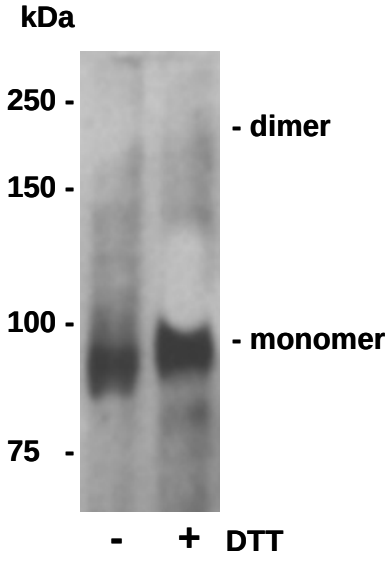

Supplementary Fig. 7| Failure to observe a TRPC5 dimer under non-reducing conditions. Western blot showing detection of TRPC5 by anti-TRPC5 antibody (T5C3) in lysates from cells expressing wild-type TRPC5. The experiment was conducted with or without DTT. The predicted mass of TRPC5 monomer is 110 kDa. Dimer (220 kDa) was not detected.

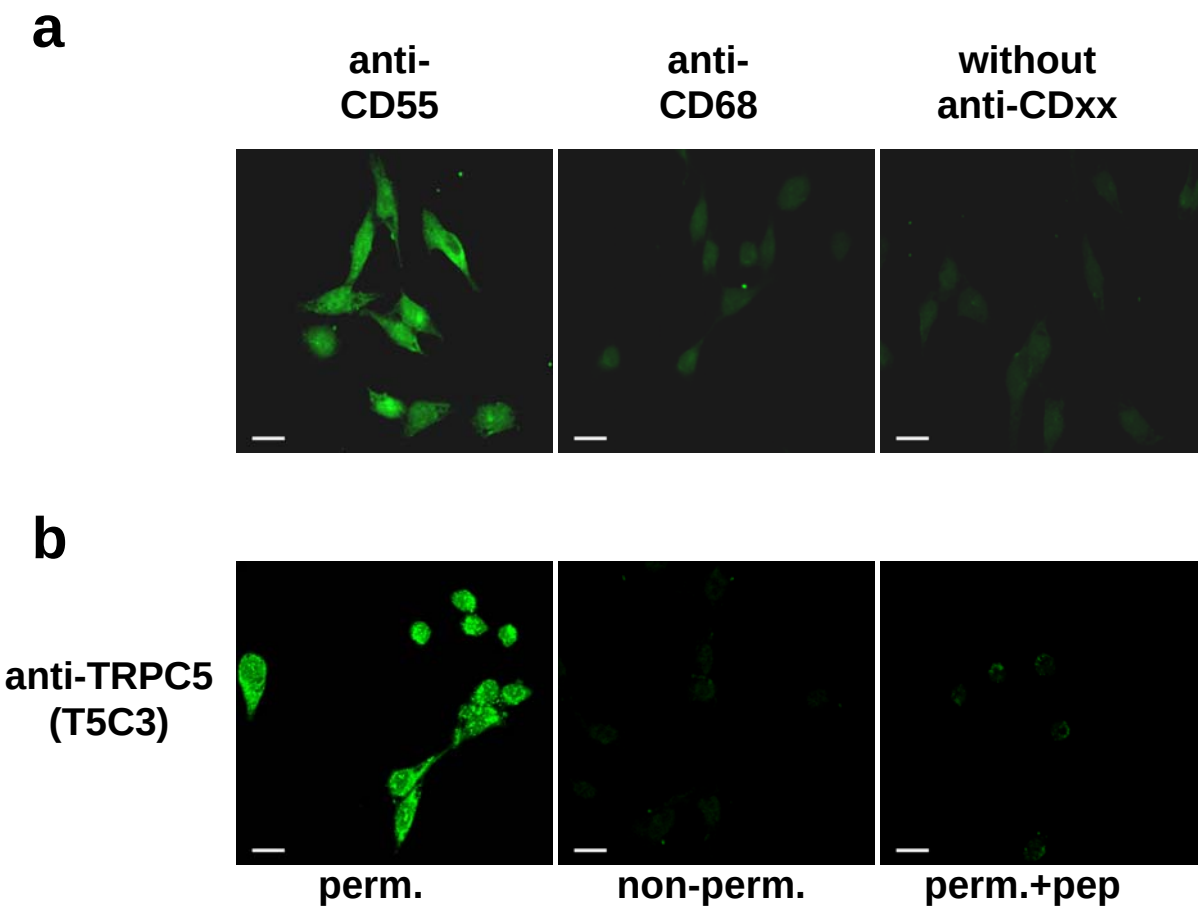

Supplementary Fig. 8| Additional evidence for TRPC5 expression in FLS cells and validation of the cell permeabilisation protocol. Immunofluorescence images from rabbit FLS cells. **a**, Labelling with anti-CD55, anti-CD68 or in the absence of either primary antibody (as a control). CD55 and CD68 are markers for fibroblast-like and macrophage-like synoviocytes respectively[11]. **b**, Labelling with T5C3, an antibody targeted to the intracellular C-terminus of TRPC5[4]. Note that staining was absent when cells were unpermeabilised (i.e. not treated with Triton X100) or T5C3 was preadsorbed to its antigenic peptide ('+pep.'). Lack of staining in unpermeabilised cells confirms that intracellular targets are not available to externally-applied antibodies under this condition, supporting the conclusion that T5E3 and T1E3 antibodies target extracellular epitopes (Supplementary Fig. 11). Scale bars are 20 μm. *Note*: We do not exclude that TRPC4 may be expressed but we have not found a reliable antibody to this protein in order to test convincingly if it is present.

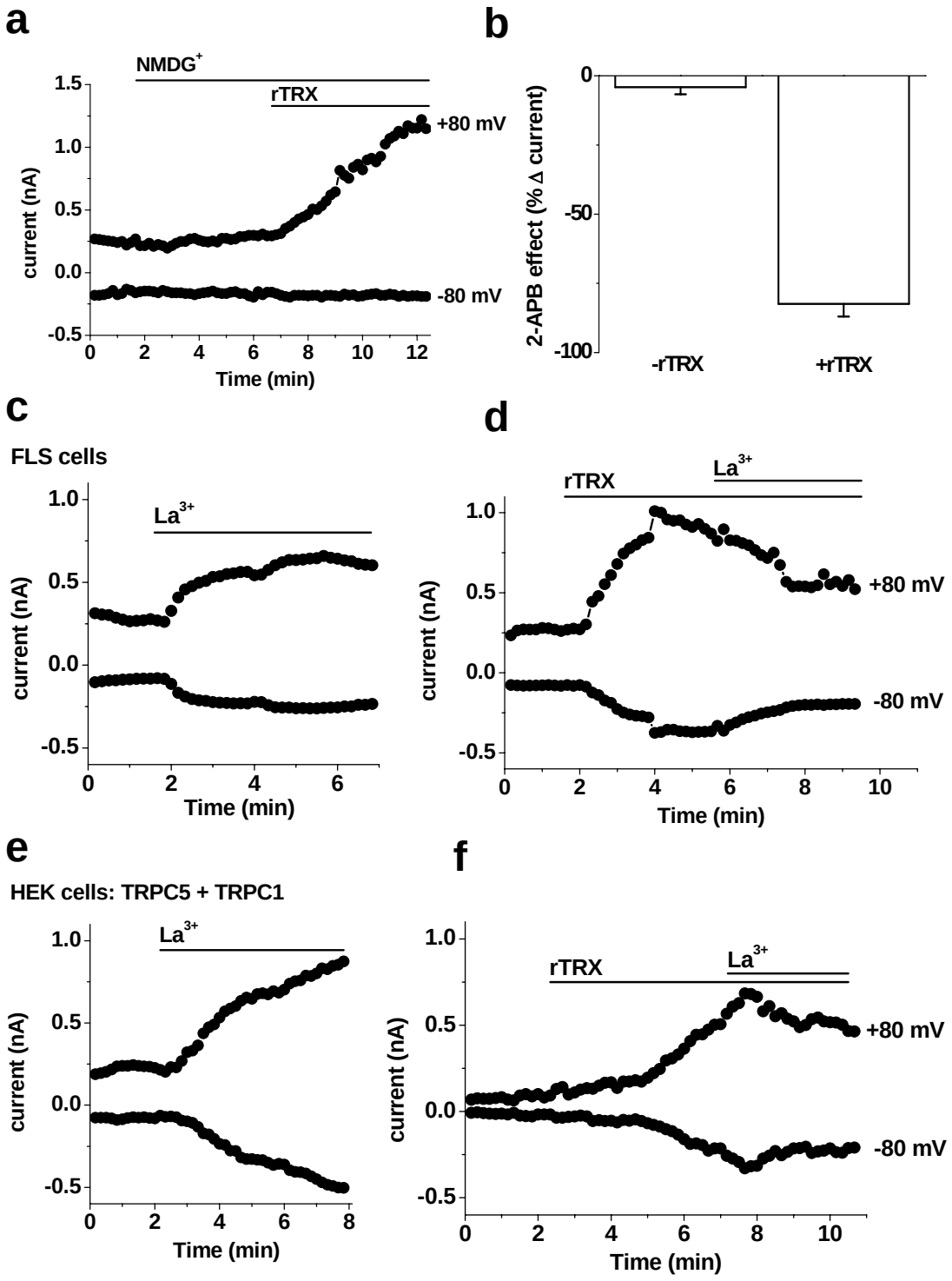

Supplementary Fig. 9| Properties of the FLS cell current. Whole-cell voltage-clamp recordings were from rabbit FLS cells (**a**-**d**) or HEK 293 cells expressing TRPC5 and TRPC1 (**e**-**f**). **a**, Time-series showing typical current evoked by 4 μg.ml^{-1} rTRX in bath solution

containing (mM): 5 NaCl, 130 NMDG (N-methyl-D-glucamine), 0.5 KCl, 8 D-glucose, 10 HEPES, 1.2 $MgCl_2$ and 1.5 $CaCl_2$ (pH was titrated to 7.4 using HCl). A typical I-V for the induced current is shown in Fig 2e. The mean reversal potential for 3 independent experiments was -76.4±1.8 mV after correction for a liquid junction potential of 4.3 mV, which was measured using a free-flowing 3 M KCl electrode as the ground. Under our experimental condition, the equilibrium potential for a channel showing equal permeability to Na^+, K^+ and Cs^+ (and no other ions) is -79.5 mV, calculated using the Nernst equation. The difference between the calculated and measured values may be explained by Ca^{2+} permeability. **b**, Inhibition of current by 75 μM 2-APB after treatment with rTRX (+rTRX) but not before (-rTRX). **c**-**f**, Typical time-series plots underlying the mean data of Fig 3c. Shown are responses to bath-applied 10 μM lanthanum (La^{3+}) before (left: **c**, **e**) or after (right: **d**, **f**) application of 4 $\mu g.ml^{-1}$ rTRX.

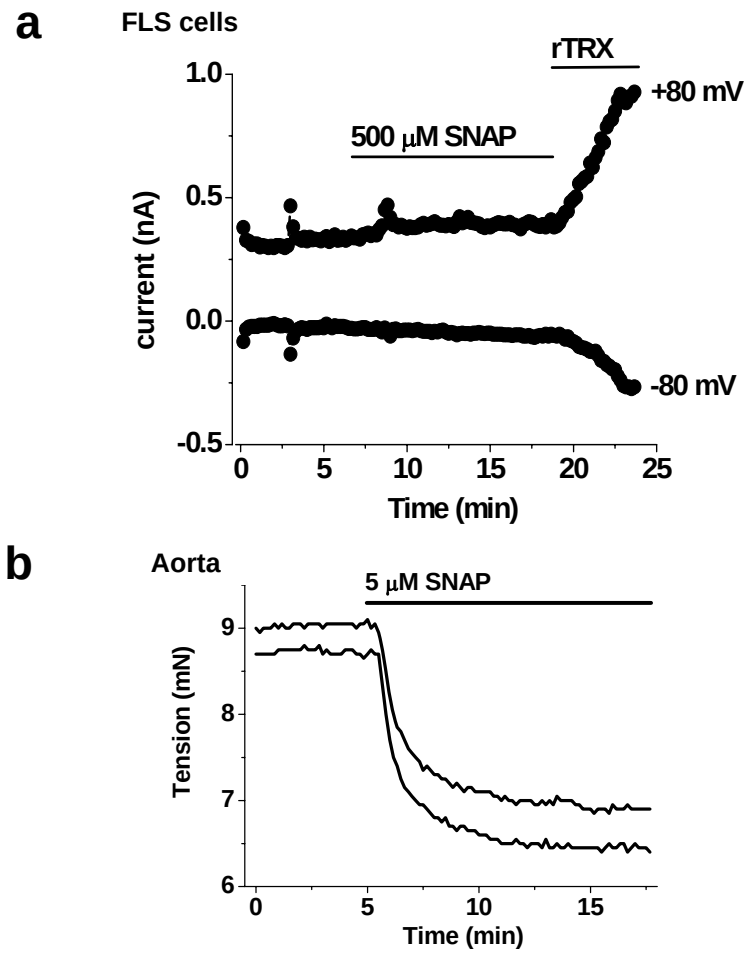

Supplementary Fig. 10| The nitric oxide donor, SNAP, does not induce current in FLS cells. a, Lack of effect of bath-applied 500 μM SNAP on ionic current recorded from a rabbit FLS cell that subsequently responded to 4 $\mu g.ml^{-1}$ rTRX. The mean current evoked by a 10 min exposure to 500 μM SNAP at -80 mV was 0.001±0.004 nA compared with 0.115±0.050 nA for the subsequent rTRX response (*n*=3 for each). SNAP at 5 μM (*n*=4) or 300 μM (*n*=3) also had no significant effect (data not shown). **b**, Relaxation of isometric tension evoked by 5 μM SNAP in two rings of mouse aorta.

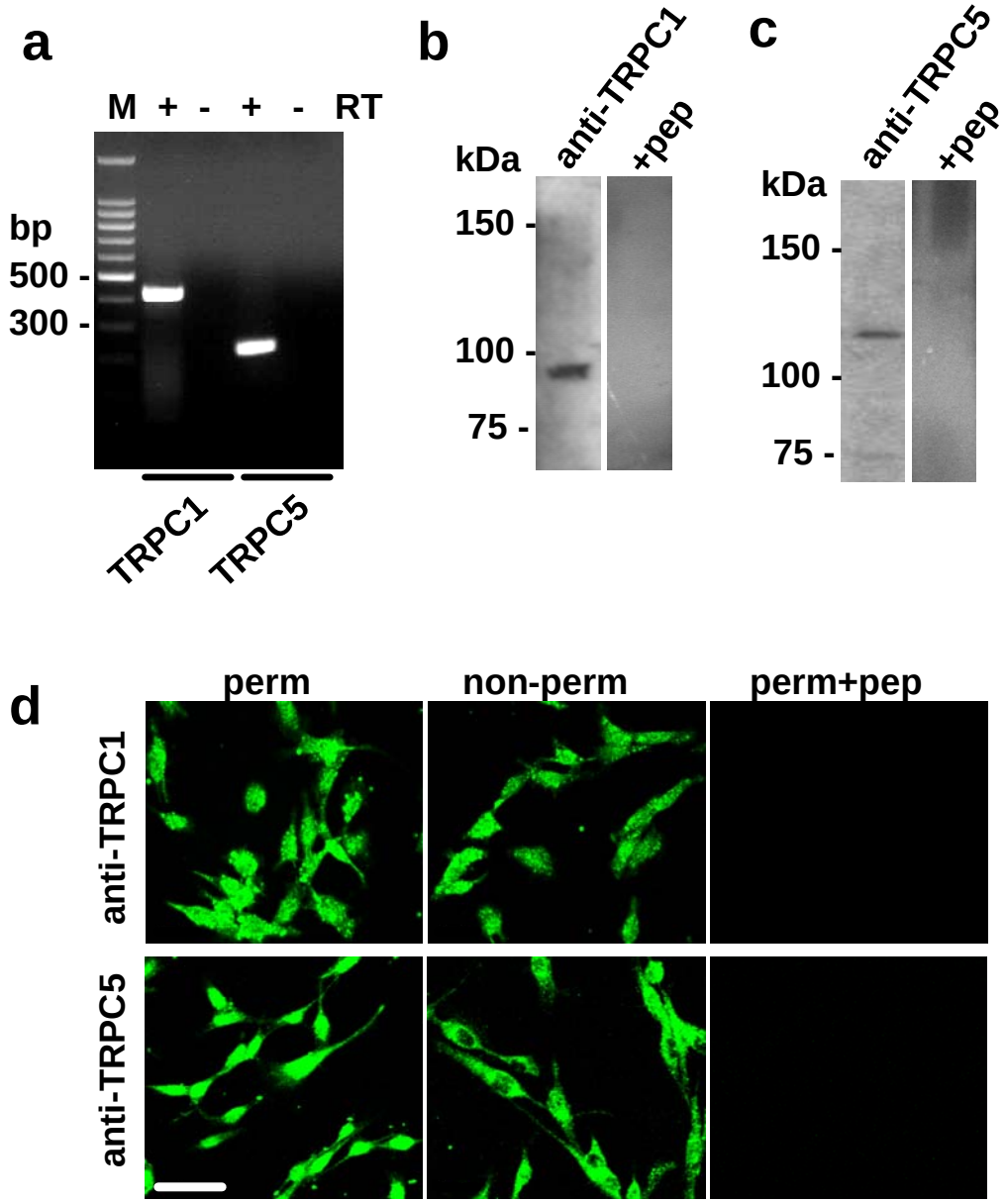

Supplementary Fig. 11| Expression of TRPC5 and TRPC1 in rabbit FLS cells. a, Gel electrophoresis showing products from RT-PCR analysis of RNA isolated from the cells. Parallel reactions were performed with (+) or without (-) reverse transcriptase (RT). Expected

sizes of the products were 423 bp (TRPC1) and 213 bp (TRPC5). **b, c**, Western blotting for cell proteins, showing single protein bands labelled by anti-TRPC1 (**b**, T1E3) or anti-TRPC5 (**c**, T5E3) antibodies. Predicted masses of TRPC1 and TRPC5 are 90 and 110 kDa respectively. Labelling was absent when antibodies were preadsorbed to their antigenic peptides (+pep). **d,** Immunofluorescence images from cells labelled with T5E3 or T1E3 antibodies with and without prior permeabilisation of the membrane. The scale bar is 40 μm.

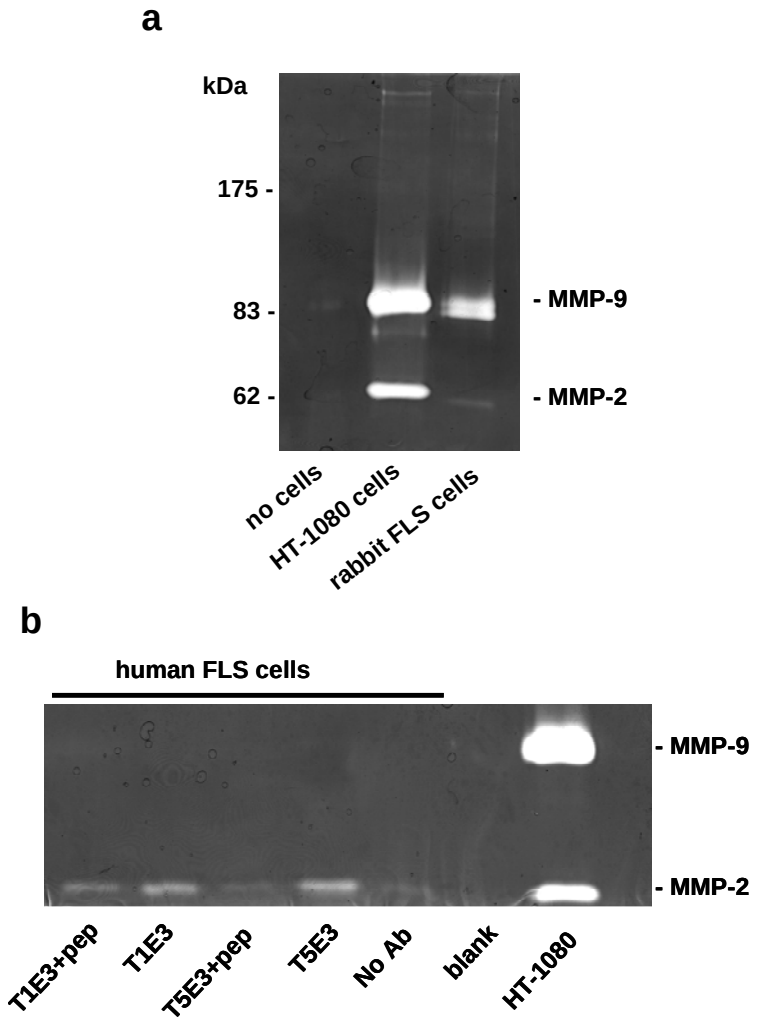

Supplementary Fig. 12| Zymography on supernatant from FLS cells. **a**, Conditioned medium from HT-1080 cells (a human fibrosarcoma cell line that constitutively secretes MMP-2 and MMP-9) was used as a positive control, and distilled water was the negative control. Rabbit FLS cells were used. **b**, Typical zymogram showing secretion of MMP-2 from human FLS cells. Antibodies to TRPC5 (T5E3) or TRPC1 (T1E3) increased MMP-2 secretion, but not if preadsorbed to their antigenic peptides.

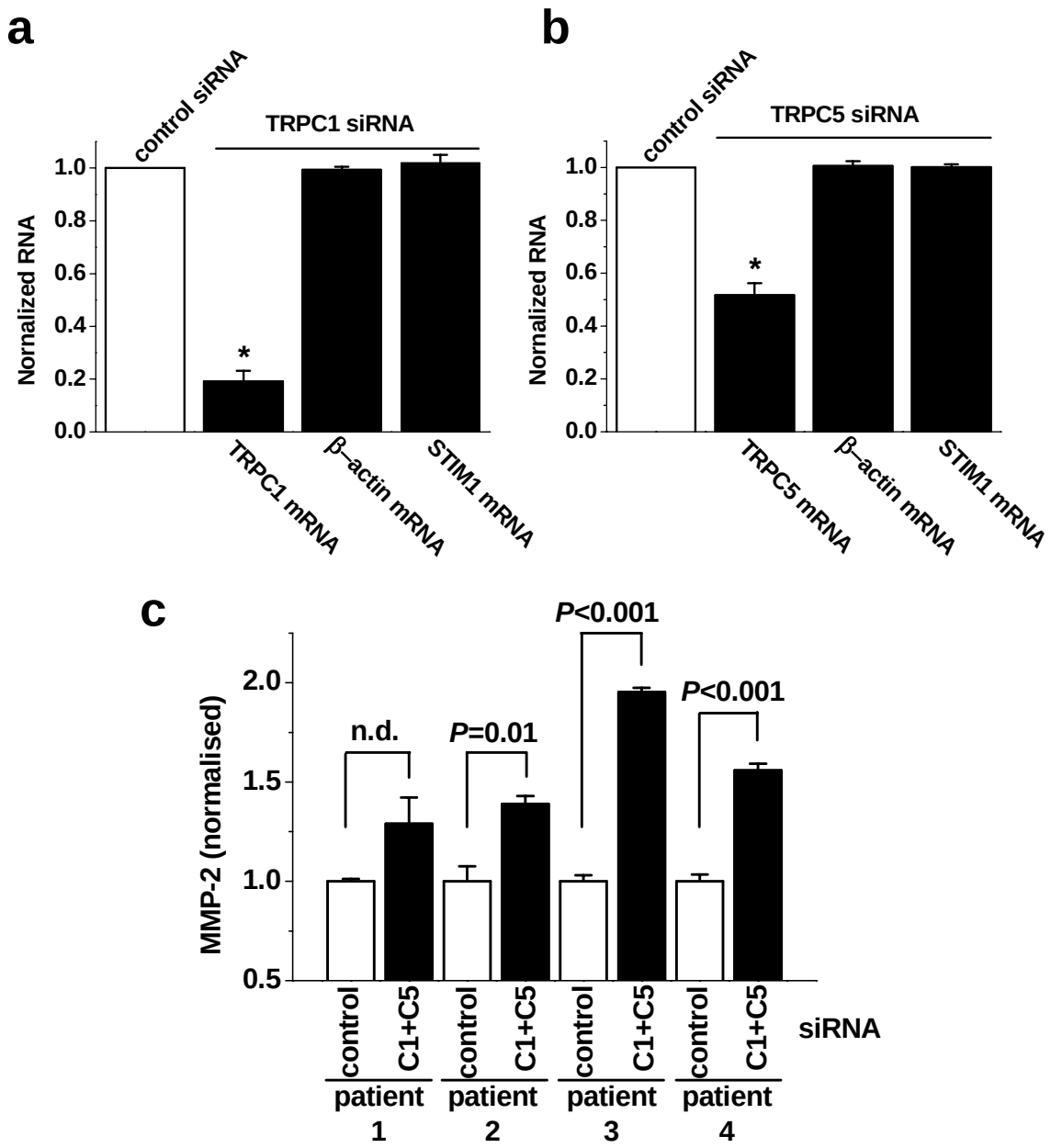

Supplementary Fig. 13| Confirmation of TRPC1/5 function using siRNA. a, b, Real-time RT-PCR data from human FLS cells validating effectiveness and specificity of the TRPC1 (**a**) and TRPC5 (**b**) siRNA probes. For each mRNA species indicated, RNA abundance after siRNA treatment was normalised to its abundance in the parallel control siRNA experiment. Reactions were performed in triplicate. STIM1 is structurally unrelated to TRP channels but is suggested to be involved in similar Ca^{2+}-entry processes. **c,** Triplicate ELISA measurements of MMP-2 secretion from FLS cells from 4 patients comparing control siRNA

and TRPC1+TRPC5 siRNA groups. TRPC1/5 siRNAs significantly increased MMP-2 secretion in cells from 3 patients. In the cells of Patient 1 there appeared to be increased secretion but the *P* value was 0.09. Combination of all 4 data sets yielded a statistically significant difference. Low transfection efficiency, incomplete knock-down and slow turn-over rates of TRPC proteins may account for the effects being smaller than those with anti-TRPC antibodies.

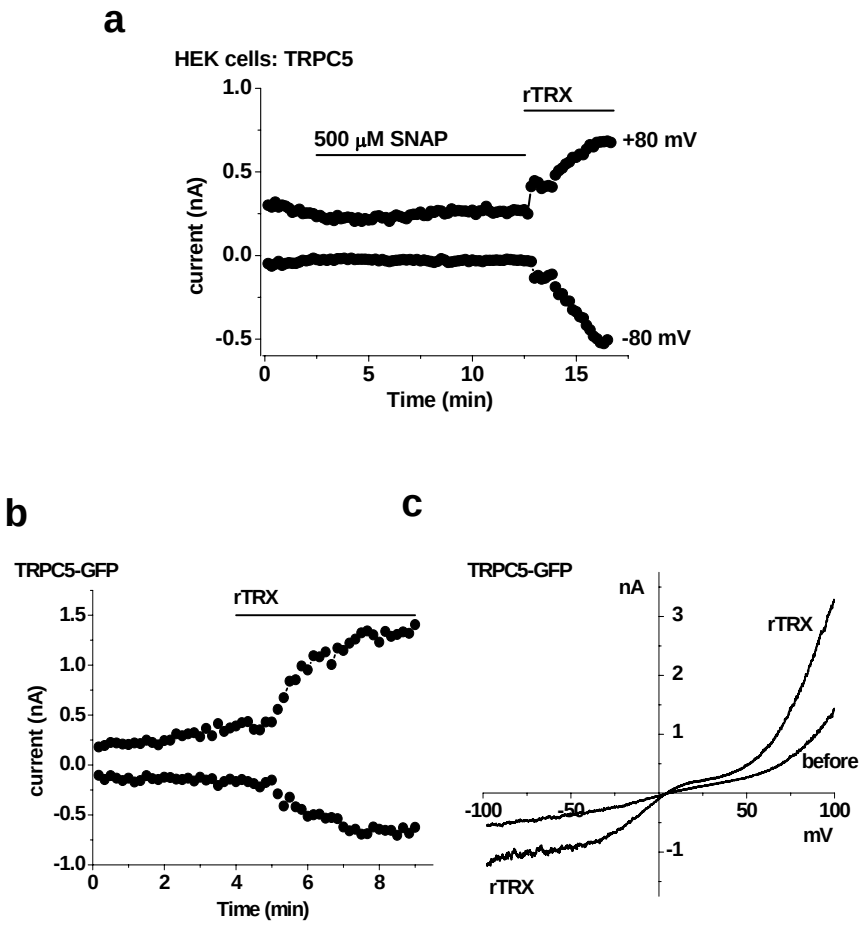

Supplementary Fig. 14| Induction of TRPC5 current by rTRX but not SNAP. Whole-cell voltage-clamp recordings from HEK 293 cells. **a,** A cell expressing wild-type TRPC5 (Tet+). Bath-applied 500 μM SNAP had relatively little effect, where as 4 $\mu g.ml^{-1}$ rTRX evoked substantial current at -80 and +80 mV. The mean current evoked by a 10 min exposure to 500 μM SNAP at -80 mV was 0.030±0.021 nA (n.d.) compared with 0.444±0.065 nA (P<0.05) for the subsequent rTRX response (n=5 for each). **b**, A cell expressing human TRPC5-GFP (wild-type TRPC5 with a C-terminal GFP tag), showing an example time-series for the effect of 4 $\mu g.ml^{-1}$ rTRX. GFP is green fluorescent protein. **c**, rTRX induced I-V for the experiment shown in (**b**).

SUPPLEMENTARY RESULTS AND DISCUSSION

A study[12] suggested intracellular nitric oxide activates TRPC5 via S-nitrosylation of C553 or C558. The conclusion was based on calcium measurement studies of TRPC5 mutants which showed that activation in response to the nitric oxide donor SNAP is absent when C553 or C558 is mutated to serine. However, by using electrophysiology we reveal that such mutants are already constitutively active and unable to be activated by agonists such as lanthanum or DTT (Fig. 1g). Therefore, lack of responsiveness of these mutants to SNAP would seem unsafe grounds to conclude that C553 and C558 are available and functionally relevant to effects of nitric oxide. Unfortunately, we cannot explore the SNAP effect further because we observe no significant activating effect of SNAP in electrophysiological experiments (Supplementary Fig. 14), despite testing a similar high concentration of SNAP as used previously[12] and demonstrating that our SNAP is a potent vasodilator (Supplementary Fig. 10), as expected for a nitric oxide donor. Like Yoshida et al[12] we observe intracellular Ca^{2+} signals in response to 0.5 mM SNAP or 0.1-1 mM hydrogen peroxide in TRPC5 expressing cells, but these are modest and slowly-developing (data not shown). Therefore, we do not exclude regulation of TRPC5 by reactive nitrogen or oxygen species, but high concentrations are needed and electrophysiological experiments clearly show priority for responses to rTRX (Supplementary Fig. 10 and Fig. 14).

Yoshida et al[12] used a GFP-tagged TRPC5 and it is conceivable that addition of the large GFP protein distorted the structure or function of the channel. We therefore prepared TRPC5-GFP and studied its electrophysiology. As for wild-type TRPC5, there is striking activation by rTRX (Supplementary Fig. 14).

Yoshida et al[12] found evidence that the reactive disulphide DTNB binds C553, suggesting this cysteine residue can be available and thus not always in a disulphide bridge.

We nevertheless would have expected the reactive disulphide to bind C558 or one of the many other cysteine residues in TRPC5. Although Yoshida et al[12] recognised that functional antibody data[8] support the location of TRPC5's "turret" in the extracellular space, they argued that the loop may dip into the channel structure under some conditions. This may be possible, but consideration should also be given to an alternative hypothesis whereby S-nitrosylation occurs at a combination of N- or C-terminal cysteine residues, by analogy with cysteine modification effects in TRPA1[13]. Such a hypothesis would be consistent with proposed mechanisms for TRPV1 sensitisation by oxidation and reduction[14].

Recent studies suggest hydrogen peroxide can inactivate thioredoxin reductase[15]. Whether hydrogen peroxide concentrations of the joints become high enough to negate the thioredoxin system is unknown but if they did, TRPC1/5 channels may remain active because of the two types of suggested TRPC1/5 activation: One is the central concept of our study where thioredoxin, thioredoxin reductase and reduced thioredoxin concentrations become elevated extracellularly such that there is TRPC1/5 stimulation via cleavage of the bridge in TRPC5. We suggest this is the dominant mechanism and it is consistent with analysis of the baseline thioredoxin system of patients with rheumatoid arthritis[15]. However, it is conceivable there are also circumstances when reactive oxygen or nitrogen species elevate sufficiently to compromise the thioredoxin system, but then activate TRPC1/5 independently of the bridge. In either situation there would be activation of TRPC1/5 channels and suppression of secretion.

SUPPLEMENTARY REFERENCES

1. Boulay, G. Ca^{2+}-calmodulin regulates receptor-operated Ca^{2+} entry activity of TRPC6 in HEK-293 cells. *Cell Calcium* **32**, 201-7 (2002).
2. Mei, Z. Z., Xia, R., Beech, D. J. & Jiang, L. H. Intracellular coiled-coil domain engaged in subunit interaction and assembly of melastatin-related transient receptor potential channel 2. *J Biol Chem* **281**, 38748-56 (2006).
3. Xu, S. Z. & Beech, D. J. TrpC1 is a membrane-spanning subunit of store-operated Ca^{2+} channels in native vascular smooth muscle cells. Circ Res 88, 84-7 (2001).
4. Xu, S. Z. et al. A sphingosine-1-phosphate-activated calcium channel controlling vascular smooth muscle cell motility. *Circ Res* **98**, 1381-9 (2006).
5. Fountain, S. J. et al. Functional up-regulation of KCNA gene family expression in murine mesenteric resistance artery smooth muscle. J Physiol 556, 29-42 (2004).
6. Strubing, C., Krapivinsky, G., Krapivinsky, L. & Clapham, D. E. TRPC1 and TRPC5 form a novel cation channel in mammalian brain. *Neuron* **29**, 645-55 (2001).
7. Doyle, D. A. et al. The structure of the potassium channel: molecular basis of K^+ conduction and selectivity. Science 280, 69-77 (1998).
8. Xu, S. Z. et al. Generation of functional ion-channel tools by E3 targeting. *Nat Biotechnol* **23**, 1289-93 (2005).
9. Jung, S. et al. Lanthanides potentiate TRPC5 currents by an action at extracellular sites close to the pore mouth. *J Biol Chem* **278**, 3562-71 (2003).
10. Obukhov, A. G. & Nowycky, M. C. A cytosolic residue mediates Mg^{2+} block and regulates inward current amplitude of a transient receptor potential channel. *J Neurosci* **25**, 1234-9 (2005).

11. Hamann, J. et al. Expression of the activation antigen CD97 and its ligand CD55 in rheumatoid synovial tissue. *Arthritis Rheum* **42**, 650-8 (1999).

12. Yoshida, T. et al. Nitric oxide activates TRP channels by cysteine S-nitrosylation. *Nat Chem Biol* **2**, 596-607 (2006).

13. Hinman, A., Chuang, H. H., Bautista, D. M. & Julius, D. TRP channel activation by reversible covalent modification. *Proc Natl Acad Sci U S A* **103**, 19564-8 (2006).

14. Susankova, K., Tousova, K., Vyklicky, L., Teisinger, J. & Vlachova, V. Reducing and oxidizing agents sensitize heat-activated vanilloid receptor (TRPV1) current. *Mol Pharmacol* 70, 383-94 (2006).

15. Lemarechal, H. et al. Impairment of thioredoxin reductase activity by oxidative stress in human rheumatoid synoviocytes. Free Radic Res 41, 688-98 (2007).